

# The Outer Tracker Detector of the HERA-B Experiment

## Part II: Front-End Electronics

### HERA-B Outer Tracker Group

H. Albrecht<sup>h</sup>, M. Bahte<sup>h</sup>, Th. S. Bauer<sup>a,q</sup>, M. Beck<sup>p</sup>,  
 K. Berkhan<sup>r</sup>, G. Boehm<sup>r</sup>, M. Bruinsma<sup>a,q</sup>, T. Buran<sup>o</sup>,  
 M. Capeans<sup>h</sup>, B. X. Chen<sup>d</sup>, H. Deckers<sup>e</sup>, X. Dong<sup>c</sup>,  
 R. Eckmann<sup>b</sup>, D. Emelianov<sup>h</sup>, G. Evgrafov<sup>h,s</sup>, I. Golutvin<sup>g</sup>,  
 M. Hohlmann<sup>h</sup>, K. Höpfner<sup>h</sup>, W. Hulsbergen<sup>a</sup>, Y. Jia<sup>c</sup>,  
 C. Jiang<sup>c</sup>, H. Kapitza<sup>f</sup>, S. Karabekyan<sup>h</sup>, Z. Ke<sup>c</sup>,  
 Y. Kiryushin<sup>g</sup>, H. Kolanoski<sup>e,\*</sup>, S. Korpar<sup>k,m</sup>, P. Križan<sup>k,ℓ</sup>,  
 D. Krücker<sup>e</sup>, A. Lanyov<sup>g</sup>, Y. Q. Liu<sup>d</sup>, T. Lohse<sup>e</sup>, R. Loke<sup>e</sup>,  
 R. Mankel<sup>e</sup>, G. Medin<sup>e,5</sup>, E. Michel<sup>h</sup>, A. Moshkin<sup>g</sup>, J. Ni<sup>d</sup>,  
 S. Nowak<sup>r</sup>, M. Ouchrif<sup>a,q</sup>, C. Padilla<sup>h</sup>, R. Pernack<sup>p</sup>,  
 A. Petrukhin<sup>h,n</sup>, M. Pohl<sup>r</sup>, D. Pose<sup>g,j</sup>, D. Rensing<sup>h</sup>,  
 B. Schmidt<sup>h</sup>, W. Schmidt-Parzefall<sup>i</sup>, A. Schreiner<sup>r</sup>,  
 H. Schröder<sup>h,p</sup>, U. Schwanke<sup>r</sup>, A. S. Schwarz<sup>h</sup>, I. Siccama<sup>h</sup>,  
 S. Solunin<sup>g</sup>, S. Somov<sup>h</sup>, V. Souvorov<sup>r</sup>, A. Spiridonov<sup>r,n</sup>,  
 M. Starič<sup>k</sup>, C. Stegmann<sup>r,e</sup>, O. Steinkamp<sup>a</sup>, N. Tesch<sup>h</sup>,  
 I. Tsakov<sup>h,t</sup>, U. Uwer<sup>e,j</sup>, S. Vassiliev<sup>g</sup>, D. Vishnevsky<sup>g</sup>,  
 I. Vukotic<sup>e,r,5</sup>, M. Walter<sup>r</sup>, J. J. Wang<sup>d</sup>, Y. M. Wang<sup>d</sup>,  
 H. J. Wilczek<sup>r</sup>, R. Wurth<sup>h</sup>, J. Yang<sup>d</sup>, Z. Zheng<sup>c</sup>, Z. Zhu<sup>c</sup>,  
 R. Zimmermann<sup>p</sup>

<sup>a</sup>NIKHEF, Kruislaan 409, PO Box 41882, 1009 DB Amsterdam, Netherlands<sup>1</sup>

<sup>b</sup>University of Texas at Austin, Department of Physics, RLM 5.208, Austin TX  
78712-1081, USA<sup>2</sup>

<sup>c</sup>Institute of High Energy Physics, Beijing 100039, China

<sup>d</sup>Institute of Engineering Physics, Tsinghua University, Beijing 100084, P.R.  
China

<sup>e</sup>Institut für Physik, Humboldt Universität zu Berlin, D-12489 Berlin, Germany<sup>3</sup>

<sup>f</sup>Institut für Physik, Universität Dortmund, D-4427 Dortmund, Germany<sup>3</sup>

<sup>g</sup>*Joint Institute for Nuclear Research, Dubna, RU-141980, Russia*

<sup>h</sup>*DESY, D-22607 Hamburg, Germany*

<sup>i</sup>*Institut für Experimentalphysik, Universität Hamburg, D-22761 Hamburg, Germany<sup>3</sup>*

<sup>j</sup>*Physikalisches Institut, Universität Heidelberg, D-69120 Heidelberg, Germany<sup>3</sup>*

<sup>k</sup>*Jozef Stefan Institute, 1001 Ljubljana, Slovenia*

<sup>l</sup>*University of Ljubljana, 1001 Ljubljana, Slovenia*

<sup>m</sup>*University of Maribor, 2000 Maribor, Slovenia*

<sup>n</sup>*Institute of Theoretical and Experimental Physics, 117259 Moscow, Russia*

<sup>o</sup>*Institute of Physics, University of Oslo, Norway<sup>4</sup>*

<sup>p</sup>*Fachbereich Physik, Universität Rostock, D-18051 Rostock, Germany<sup>3</sup>*

<sup>q</sup>*Universiteit Utrecht/NIKHEF, 3584 CB Utrecht, The Netherlands<sup>1</sup>*

<sup>r</sup>*DESY, D-15738 Zeuthen, Germany*

<sup>s</sup>*visitor from Moscow Physical Engineering Institute, 115409 Moscow, Russia*

<sup>t</sup>*visitor from Institute for Nuclear Research, INRNE-BAS, Sofia, Bulgaria*

<sup>u</sup>*visitor from Yerevan Physics Institute, Yerevan, Armenia*

---

## Abstract

The HERA-B Outer Tracker is a large detector with 112 674 drift chamber channels. It is exposed to a particle flux of up to  $2 \cdot 10^5 \text{ cm}^{-2} \text{ s}^{-1}$  thus coping with conditions similar to those expected for the LHC experiments. The front-end readout system, based on the ASD-8 chip and a customized TDC chip, is designed to fulfil the requirements on low noise, high sensitivity, rate tolerance, and high integration density.

The TDC system is based on an ASIC which digitizes the time in bins of about 0.5 ns within a total of 256 bins. The chip also comprises a pipeline to store data from 128 events which is required for a deadtime-free trigger and data acquisition system.

We report on the development, installation, and commissioning of the front-end electronics, including the grounding and noise suppression schemes, and discuss its performance in the HERA-B experiment.

*Key words:* HERA-B experiment, drift chamber, drift tubes, readout electronics, TDC

*PACS:* 29.40.Gx

---

---

\* Corresponding address: DESY, Platanenallee 6, D-15738 Zeuthen, Germany, Tel.: +49-33762-77380, fax: +49-33762-77330.

*Email address:* `hermann.kolanoski@desy.de` (H. Kolanoski).

<sup>1</sup> Supported by the Foundation for Fundamental Research on Matter (FOM), 3502 GA Utrecht, The Netherlands

<sup>2</sup> Supported by the U.S. Department of Energy (DOE)

<sup>3</sup> Supported by Bundesministerium für Bildung und Forschung, FRG, under contract numbers 05-7BU35I, 05-7D055P, 05 HB1KHA, 05 HB1HRA, 05 HB9HRA, 05 7HD15I, 05 7HH25I

<sup>4</sup> Supported by the Norwegian Research Council

<sup>5</sup> Supported by German Research Foundation (Research Training Group GK 271)

## 1 Introduction

HERA-B was designed as a fixed target experiment for studying CP violation in  $B$ -meson systems using an internal wire target in the proton beam of HERA [1]. To reach the necessary production rate of  $b$  quarks an average of four interactions per bunch crossing at a frequency of about 10 MHz (96 ns bunch separation) has to be generated. This leads to a very high particle flux density in the detector.

The main detector components (fig. 1) are a silicon vertex detector, a dipole magnet with a field integral of 2.13 Tm, a main tracker with an Inner Tracker composed of microstrip gas chambers and an Outer Tracker composed of drift tubes, High- $p_T$  Chambers, a ring imaging Cherenkov counter (RICH), an electromagnetic calorimeter (ECAL), and a Muon System with drift tubes. The detector covers a forward angular range of 220 mrad in the bending plane of the magnet and 160 mrad vertically.

In the following we describe the front-end electronics of the Outer Tracker drift tubes, i. e. the outer part of the main tracking system, which is based on the amplifier-shaper-discriminator chip ASD-8 [2] and a TDC (time-to-digital-converter) chip customized for HERA-B.

The paper is organized as follows: in the next section the Outer Tracker detector is briefly described followed in section 3 by a discussion of the design considerations for the front-end electronics. The sections 4 to 6 contain the description of the main components of the front-end electronics: the high-voltage system, the ASD8 board and the TDC board. Section 7 describes the installation and commissioning of the electronics and gives a first evaluation of the performance. The paper finishes with a summary.

## 2 The Outer Tracker System

**Detector Description:** The Outer Tracker of HERA-B [1,3] is composed of 13 planar superlayers (fig. 1) of drift tube modules comprising 112 674 readout channels. Each superlayer consists of two independent chambers. For each chamber the modules are contained in a gas-tight box which is suspended from a rigid frame ('outer frame'). Of the 13 superlayers 7 are placed in the magnet ('magnet chambers' = MC), 4 in the field-free region between the magnet and the RICH serving for pattern recognition ('pattern chambers' = PC) and 2 between the RICH and the ECAL ('trigger chambers' = TC). The two TC superlayers and the first and last PC superlayers deliver hit signals to the First Level Trigger. The main tracking system allows for momentum

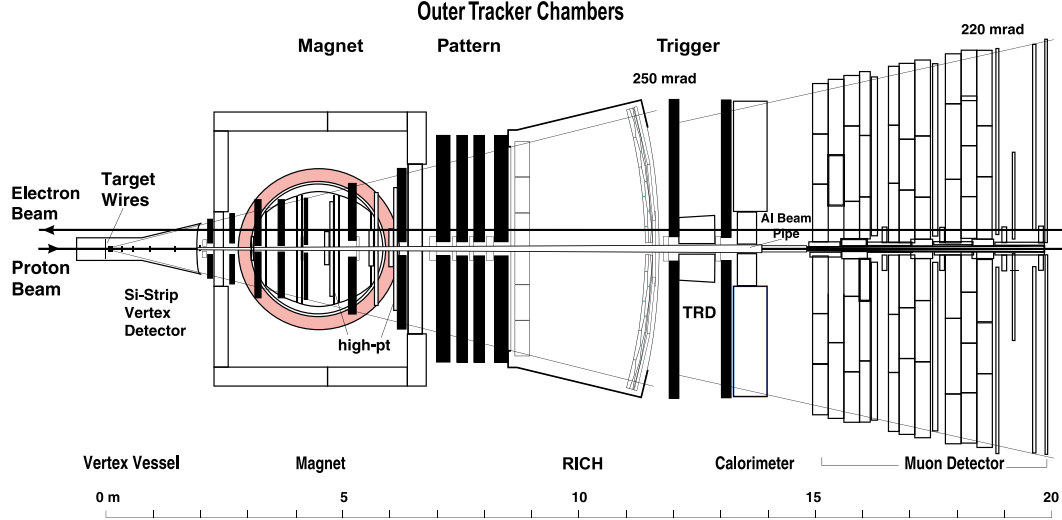


Fig. 1. Top view of the HERA-B detector. The Outer Tracker superlayers, arranged as magnet, pattern and trigger chambers, are indicated by the black areas (with the Inner Tracker modules attached to them near the beam pipe, white areas).

measurement and provides track recognition on the first trigger level.

The honeycomb modules of hexagonal drift tubes are built from folded gold-coated, carbon-loaded polycarbonate foil. The tubes are oriented at  $0^\circ$  and  $\pm 5^\circ$  relative to the perpendicular on the bending plane. In the bending plane the inner diameter of the cells changes from 5 mm near the beam to 10 mm above a certain distance from the beam (about 1 m in the PC area) to account for the radial dependence of the particle flux.

As counting gas the fast mixture  $\text{Ar}/\text{CF}_4/\text{CO}_2$  (65/30/5) is chosen. Operating at a gain of  $3 \cdot 10^4$ , the drift velocity is about  $80 \mu\text{m}/\text{ns}$  which allows the particle signals to be collected within the bunch separation time of 96 ns, even within the magnetic field. In this gas the ionisation density of a minimum ionising track is estimated to be about 100/cm with an average cluster size of 2.5 electrons. However, due to the loss of electrons by attachment only about 30% of the electrons reach the anode, leading to a mean cluster size of about 1 electron.

**Radiation load and occupancies:** The Outer Tracker has been designed for particle densities and radiation levels comparable to those in similar detectors currently developed for LHC. At an interaction rate of 40 MHz the radial distribution of the charged particle flux density is roughly given by:

$$\phi \approx \frac{10^8}{R^2} \text{ Hz}$$

where  $R$  is the distance from the beam (in any units). Since the Outer Tracker acceptance starts at a radial distance of about 19 cm to the beam this leads to a particle flux of about  $2 \cdot 10^5 \text{ cm}^{-2} \text{ s}^{-1}$  in the hottest area.

The drift tubes are longitudinally subdivided into sensitive and insensitive segments to limit the single channel occupancy to about 20% at an interaction rate of 40 MHz (the shortest segmentation near the beam is 20 cm). The subdivision is achieved by installing a sense wire only in the sensitive parts of a cell [3]. If a sensitive part is not at an end of the cell the signal is carried to the upper or lower end of the module via a thicker wire which does not generate an avalanche. The sensitive length of the drift cells,  $L_{cell}$ , varies between 0.2 m and 2.8 m yielding different cell capacities. The capacitive load at the input of the amplifier is about  $15 \text{ pF} + L_{cell} \cdot 10 \text{ pF/m}$ , resulting in loads between 17 and 43 pF.

The amplifiers are placed at the upper or lower end of the chambers, away from the beam pipe at a location where the radiation load is below 50 Gy per year. The TDC electronics is installed on the outer frames, at an even lower radiation level.

### 3 Design Criteria for the Front-End Electronics

The performance of the front-end electronics influences the drift chamber resolution, the detection efficiency and the rate of noise hits. In the following we discuss the considerations which led to the definition of requirements for the Outer Tracker electronics.

#### 3.1 Requirements on the Front-End Electronics

A good position resolution of the drift chamber hits is not only needed for a precise momentum measurement, but in a dense particle environment it also facilitates the pattern recognition. For the Outer Tracker it was estimated that the resolution should be about  $200 \mu\text{m}$  [1].

In order to achieve this for the given cylindrical drift tube geometry and the ionisation density of the chosen gas the electronics should be able to trigger on the first cluster of electrons arriving at the anode. The charge signal generated by the electrons at the amplifier input depends on the gas gain. For safety reasons, to avoid high-voltage break-down and accelerated aging effects, it was decided to limit the gas gain to  $3 \cdot 10^4$ . With this gain an average cluster (including the attachment loss in  $\text{CF}_4$ ) results in a charge of about 2 fC after

fast shaping with a charge collection efficiency of about 20% which is typical for drift chamber electronics. With a threshold corresponding to a single electron cluster also the requirement of the First Level Trigger of a high single cell efficiency (design value  $> 98\%$ ) can be fulfilled. The efficiency should stay high for counting rates of up to about 2 MHz per cell corresponding to the maximal allowed occupancy.

Processing such small signals requires low noise and low crosstalk in the system. The noise occupancy per channel, i. e. the probability to find in a channel a noise hit in the readout window of 96 ns, should not exceed 1% to limit the amount of false data. The crosstalk of a charge signal into neighbouring channels depends on its total charge which is roughly 40 times larger than the desired threshold charge. Therefore the analog crosstalk should not exceed 1%.

The strongest demands on the amplifier bandwidth and the signal shaping come from the First Level Trigger which requires a fast signal collection within the bunch separation time of 96 ns. With a fast signal shaping also pile-up in following bunches will be reduced.

Because of the large number of channels a high integration density of the amplifiers at low power consumption is necessary. The requirements on radiation tolerance are moderate, as explained in the previous section.

For the digitization of the drift time 1 ns bins are sufficient because in this case the uncertainty of the time measurement adds only about  $25\ \mu\text{m}$  to the position resolution which is negligible when quadratically added to the intended  $200\ \mu\text{m}$ . To allow for a deadtime-less trigger and readout scheme the data have to be stored in a 128 bunch crossings deep pipeline [4].

In the design phase of the electronics, which started in 1995, the evaluation of available electronics led to the selection of the amplifier-shaper-discriminator chip ASD-8 and the decision to develop a TDC chip as the basic components of the front-end electronics.

### *3.2 Overview of the system*

The front-end electronics of the Outer Tracker (fig. 2) consists of

- a high-voltage (HV) board with coupling capacitors for the chamber signals and resistors for the current protection,
- a twisted pair cable, routing the signals to a feed-through board in the wall of the gas box,
- a feed-through board which transfers the signal through the wall of the gas

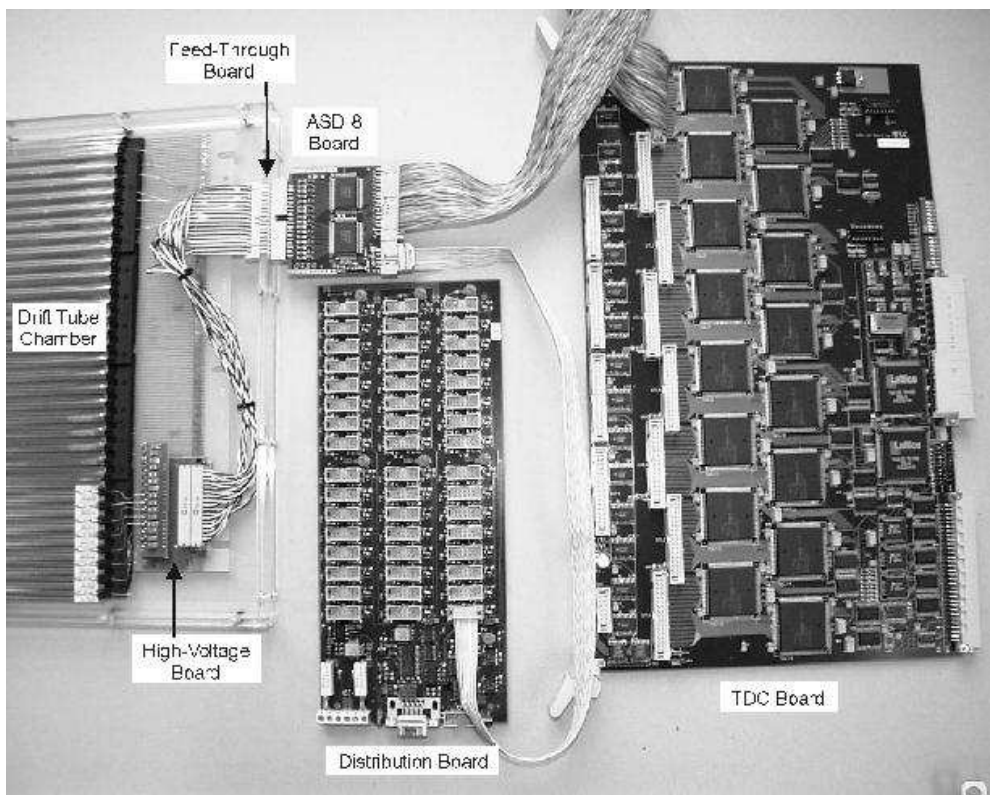
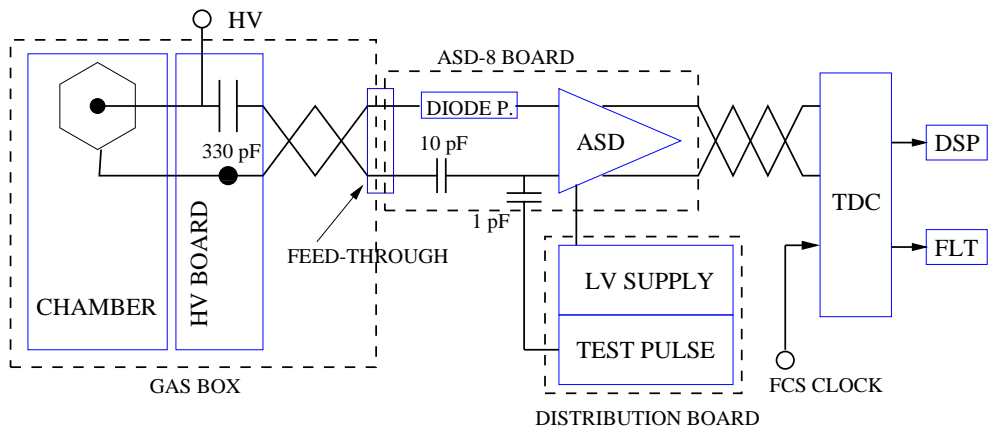


Fig. 2. The front-end electronics of the Outer Tracker (top: schematics for one channel, bottom: photograph of a demonstration assembly cabled for 16 channels).



- box and which serves as a mount for the ASD-8 board,
- an ASD-8 board,
- a low voltage distribution board to supply the ASD-8 board with power, threshold voltages, and test pulses,
- a shielded twisted pair cable from the ASD-8 board to the TDC board,
- a TDC board.

The HV boards, distributing the HV to each cell, are mounted on the modules inside the counting gas-volume where the dry gas serves as discharge protection. The other readout electronics components are mounted outside the gas box for better accessibility. The HV part includes a coupling capacitor for each channel which AC-couples the anode signals to the amplifier since the anode wires are on positive high voltage while the cathode foils are connected to the ground. The TDC boards are housed in crates on the outer frames of the superlayers which carry the cables between the ASD-8 and the TDC boards. The TDC boards are connected via electrical cables (signal standard: LVDS = Low Voltage Differential Signaling) to digital signal processors which build the front-end of the DAQ system. In addition the hit information of 4 selected superlayers (trigger layers) is transferred to trigger link boards for use in the First Level Trigger system. More information on the HERA-B trigger and data acquisition system can be found in [4].

In the following section we discuss the functionality of the listed components. More details, including the electronic schematics of the developed boards can be found in [5].

### *3.3 Grounding and Shielding*

A concept for grounding and shielding, which is essential for the performance and stability of the whole system, has been developed to minimize noise, pickup, crosstalk and signal feedback.

In the following we explain the scheme referring to fig. 3. For each superlayer half one single “ground reference point” (GND RP) is defined which is chosen to be fixed to the potential of the gas box. The ground potentials of all components have to be connected to GND RP (star-like). There is only one connection to the reference potential of the mains (Net0) via the HV power supply which, for safety reasons, had to be connected to the gas box. All other lines coming from Net0 connect only to otherwise electrically insulated parts, like the enclosures of electronics (LV, TDC), the outer frame, and the gas pipe.

The most critical points are the grounding of the analog and digital sections on the ASD-8 board, and the signal connections from the chamber to the ASD-8 board and from the ASD-8 board to the TDC. On the ASD-8 board, the digital

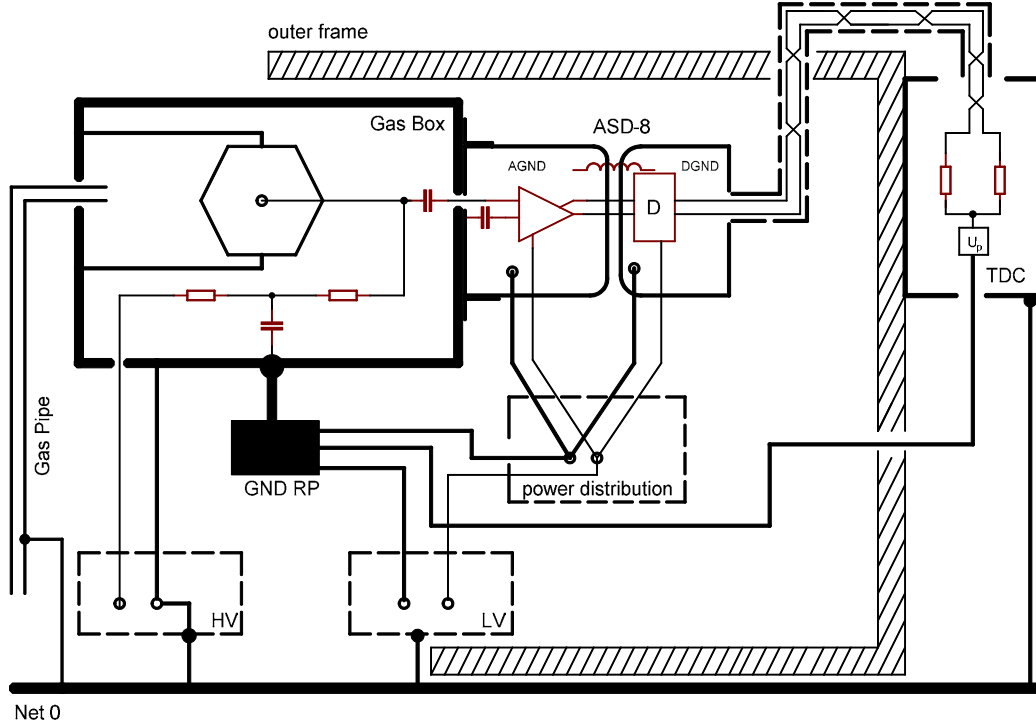


Fig. 3. Grounding scheme of the Outer Tracker front-end electronics.

ground (DGND) and the analog ground (AGND) are separated (see section 5.2). A good connection of the AGND to the cathodes is mediated by the gas box enclosing each chamber. From the inside, the cathodes are connected to the box, and from the outside Cu-Be brackets, carrying the ASD-8 boards, connect to the AGND of the board. Being designed as a Faraday cage the gas box serves also as a RF shield. It is insulated from the outer frame and from the gas pipe (using insulating pipe connections).

Shielding of the signal cables going to the TDC turned out to be absolutely necessary to minimize the feedback of the digital output signals to the amplifier inputs. The shielding is connected to DGND on the ASD-8 board without any direct ground connection from the ASD-8 board to the TDC. The ground potential on the TDC board is connected to the ground reference point GND RP.

The final tuning of the grounding and shielding of the complete system during commissioning is described in section 7.

## 4 High Voltage System

### 4.1 High Voltage and Signal Routing in the Gas Box

The high voltage is supplied to the anode wires via HV boards, which are mounted on the module base plates [3]. The schematics of the boards is shown in fig. 4. Besides supplying high voltage to individual anode wires via a 1 M $\Omega$  protection resistor, the board also leads the signals from the anode wires through coupling capacitors (330 pF, 4 kV)<sup>6</sup> to the cable connectors, leading to the ASD-8 boards. The high voltage enters the board through an RC filter (100 k $\Omega$ , 330 pF).

To accommodate the HV board to the chamber structure (fig. 4), a combination of two boards, a main board with a piggy-back board on top of it, is used (fig. 5). The main board supplies the channels 1A to 16A, the piggy-back board the remaining channels 1B to 16B. For the chambers which are not used in the First Level Trigger the signal routing is such that the channels on the main board end up in one cable and the channels from the piggy-back board in another. For trigger chambers the cabling is such that back-to-back drift cells nB and (n+2)A end up in neighbouring channels of the output cable. This routing facilitates performing a logical OR of hits from these cells in order to increase the trigger efficiency.

The HV boards are double-sided printed circuit boards with surface mounted components (SMD). For the 5 mm cells the matching to the wire pitch limits the board width to 67 mm requiring a tight spacing between the capacitors. In order to guarantee the high voltage proofness, two of the 17 HV capacitors are placed on the back side of the board (because of a different soldering method these two capacitors caused major problems in the first running period, see section 7).

The signal cables (16 twisted pairs, lengths between 25 and 50 cm) from the HV boards are plugged on the inside of the gas-box to the feed-through boards which hold on their outside the ASD-8 boards. The feed-through boards provide also the feed-through for the high voltage and a possibility to individually disable problematic HV boards.

---

<sup>6</sup> ceramic chip capacitors 330 pF, 4 kV, X7R dielectric, Johanson Dielectrics (art.nr. 402 S43 W 331 KV4)

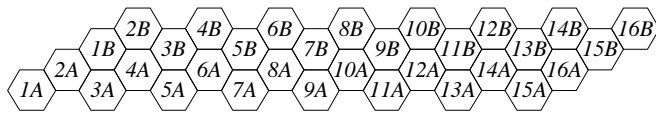
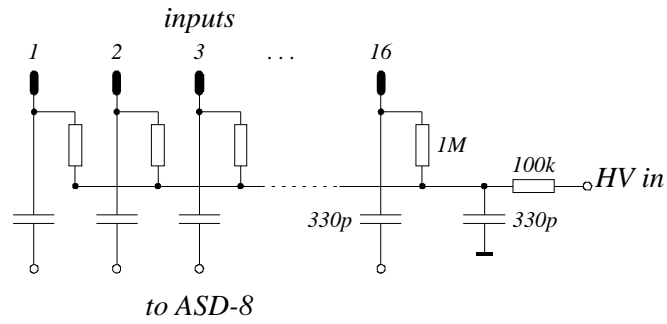


Fig. 4. High voltage distribution board: schematics (top) and board-to-chamber mapping (bottom).

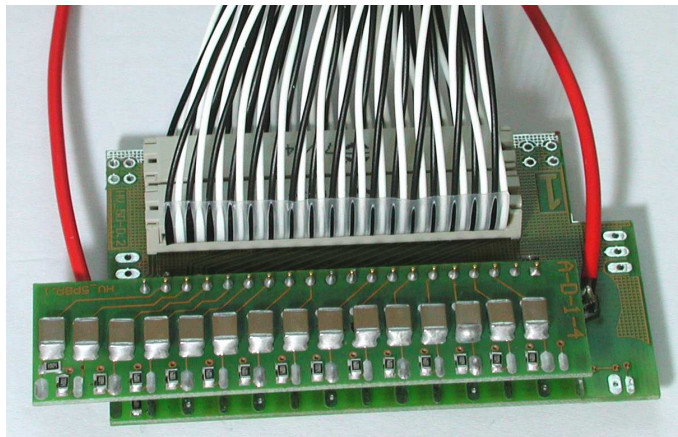


Fig. 5. High voltage distribution board: a photograph of the connected main and piggy-back boards for the 5 mm chambers.

## 4.2 *The High Voltage Distribution and Protection System*

The Outer Tracker High Voltage System has a cascaded distribution scheme which optimizes the number of dead channels in case of high voltage problems due to unstable or broken wires with respect to the cost of the system. It provides positive voltage for the 112 674 anode wires, nominally 1700 V for 5 mm drift cells and 1950 V for 10 mm cells.

The HV grouping follows the structure of the Outer Tracker which is described in [3]: The largest individual detector units are the superlayer halves, being composed of stereo layers (6 for PC and 3 for TC) which are then subdivided into sectors (12 per PC, 10 per TC stereo layer).

The HV supply system<sup>7</sup> has 160 individually controllable HV sources, each of which feeds up to six sectors with up to 1500 wires in total. Such a HV source is the smallest unit which can be monitored and controlled by the Slow Control software. However, failing single sectors can be disconnected individually on a patch board in the electronics trailer. Beyond that also the groups of 16 wires belonging to an HV board (fig. 4) can be switched off at the feed-through board on the gas box frame. This action requires an access to the detector which is regularly scheduled once per month. In this way the number of disabled channels per faulty wire can be limited to 16.

For each of the 160 HV sources the current is continuously monitored and in case of over-currents a protection scheme first reduces the voltage and eventually switches it off. An interlock makes sure that the HV can only be switched on, if the gas system works properly. To provide a constant gas gain the HV is adjusted automatically within defined limits by a gas monitor system. A description of the control system is given in [9].

## 5 **The ASD-8 Electronics**

### 5.1 *The ASD-8 Chip*

The amplifier-shaper-discriminator chip ASD-8 [2], developed by the University of Pennsylvania for drift chamber applications in a high rate environment (originally for SSC), is used in different detector systems of the HERA-B ex-

<sup>7</sup> CAEN SY527 Multichannel HV System: One crate with 10 HV Supply Boards A734P, each board with 16 HV channels (max. 3 kV/3 mA), connected to the Slow Control system via V288 HS-CAENET-VME Interface.

Table 1  
 Characteristics of the ASD-8 chip.

integration density	8 ch. on $2.7 \times 4.3 \text{ mm}^2$ die
power consumption	0.3 W / chip (incl. output)
signal shaping time	about 10 ns
tail cancellation	$t_0 \approx 1.5 \text{ ns}$
double pulse resol.	25 ns
intrinsic noise	$(900 + 70/\text{pF})$ electrons
on-chip crosstalk	analog: $\sim 0.1\%$
threshold	$\sim 2 \text{ fC}$
baseline shift	0.5 - 1.0 fC/MHz

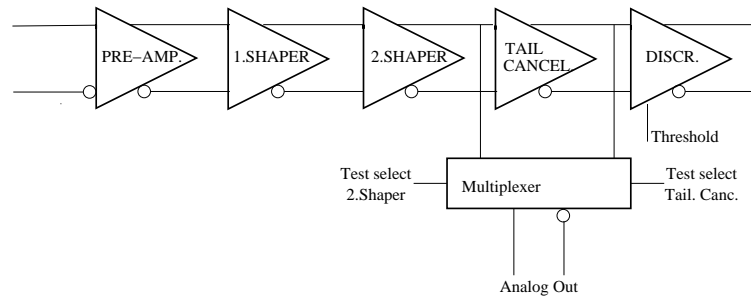


Fig. 6. Principal functions of the ASD-8 chip. The analog outputs are only used for test purposes and can be selected by an on-chip multiplexer.

periment (Outer Tracker, RICH, Muon System, High- $p_T$  Chambers) with a total of about 200 000 channels.

The 8-channel chip is designed in a bipolar technology. The process used by the producer Maxim combines high speed with a low noise level, and relatively low power consumption (Table 1).

A block diagram of the ASD-8 chip is shown in fig. 6. The input stage is a preamplifier with a sensitivity of  $2.5 \text{ mV/fC}$ , a bandwidth of 100 MHz and an input impedance of  $115 \Omega$ . The input is differential and symmetric for positive and negative pulses.

The two-stage shaper with tail cancellation yields a double pulse resolution of 25 ns. The tail cancellation compensates the ion tail of the drift chamber pulses. Analog outputs are provided for 3 channels per chip, selectable after the second shaper or after the tail cancellation.

The discriminator is a two-stage differential amplifier with positive feedback. The threshold is voltage programmable for each channel. The external voltage

Table 2  
 Technical data of the ASD-8 board

channels	16 (2 chips)
dimensions	4 layers, $67 \times 56 \text{ mm}^2$
pickup suppression	all supply voltages RC filtered
spark protection	diode protection $\geq 3 \text{ kV}$
crosstalk (analog)	$< 0.5\%$
grounding	analog - digital separated
gain uniformity	$\pm 15\%$ per board
output	2 mA into $62 \Omega$
voltage supply	+3 V, 100 mA -3 V, 100 mA
power	600 mW

scales approximately like  $250 \text{ mV} / \text{fC}$  up to about 1.4 V where the threshold saturates. The baseline shift given in Table 1 is not negligible at the highest occupancies and has to be compensated by a corresponding threshold shift. The differential, open collector output is current programmable to adjust the signal swing.

## 5.2 The ASD-8 Board

**Design considerations:** The analog inputs of the ASD-8 chips have a very high sensitivity which makes them susceptible to noise and RF pickup. Because of the combination of analog inputs and digital outputs on the chip a particular worry is the feedback from the output to the input. In the design of the printed circuit boards carrying the ASD-8 chips special care was taken for a good grounding scheme, decoupling of the analog and digital parts, noise rejection from power sources, and crosstalk separation of different channels in a densely packed environment.

Since only one board type for both the 5 mm and 10 mm cells should be produced, the geometrical constraints are defined by the dimensions of the 5 mm cells. The width of the boards was adjusted to the cell pitch; a compact assembly of connectors and electronic components was achieved using SMD technology.

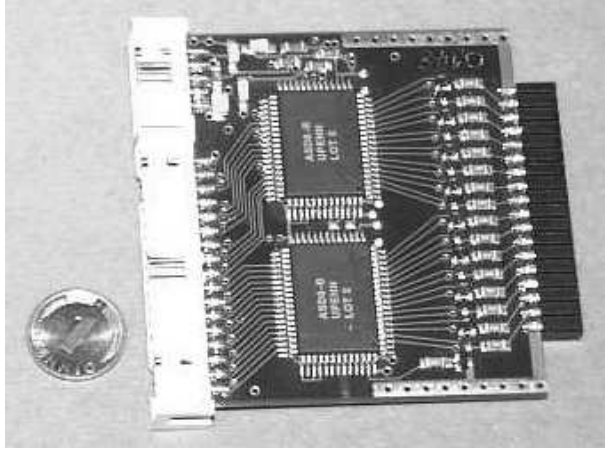


Fig. 7. Picture of the ASD-8 board of the HERA-B Outer Tracker.

**Board layout:** Two ASD-8 chips with 8 channels each are mounted on a multilayer board (Table 2, fig. 7). A block diagram of the board is shown in fig. 8, more details can be found in [5].

The chip has a differential input while the nature of the chamber signals is not differential. With the anode signal fed into the negative input different options for the positive input were tested. The best common mode rejection was obtained by connecting the positive input via 10 pF to the chamber ground, i. e. the cathode (fig. 2). This quasi-differential use of the inputs was clearly superior to the option to leave the positive input open.

All supply voltages ( $\pm 3\text{ V}$ ) are separated for the analog, digital and output drive circuits and have RC filters at the input. The ground plane is separated for the analog and digital part of the chip. Both grounds are connected via an inductance of  $10\ \mu\text{H}$ . The analog ground is extended to rails along the sides of the board which slide into the holding brackets on the chambers made of Cu-Be springs. Thus the brackets together with the ground planes provide a shielding mesh between the boards in the densely packed front-end electronics on the chambers (see fig. 9). Since it was found that the ASD-8 inputs survive voltage spikes only up to about 300 V, a diode protection circuit was added to protect against high voltage breakdowns in the drift cells. The protection circuit consists of an input resistor of  $50\ \Omega$  and two diodes connected in parallel with opposite polarity (type BAV79) shortening the ASD-8 input against a 0.7 V level [5]. Tests have shown that in this way the input transistors could be protected against discharges of 3000 V fed into the input via a 1 nF capacitor.

Only one voltage level for the thresholds is provided per board. The two chips on each board were therefore selected in order to be in the same gain and noise quality classes (defined in section 5.4.1). The maximum difference of the reference thresholds  $U_{ref}$  of two channels of a single board, as defined below, should be less than 300 mV. In some cases Schottky diodes (forward voltage



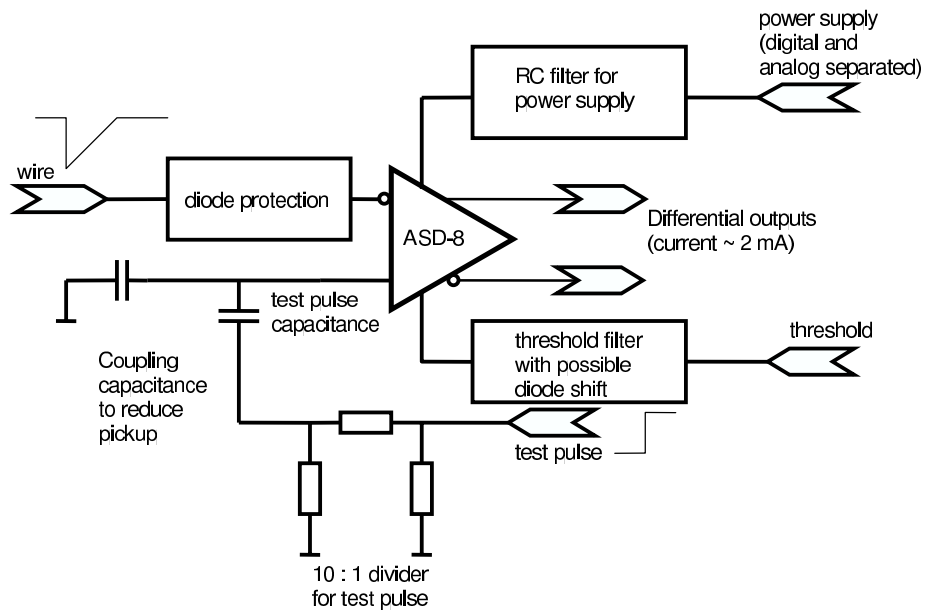


Fig. 8. Block diagram of the ASD-8 board.

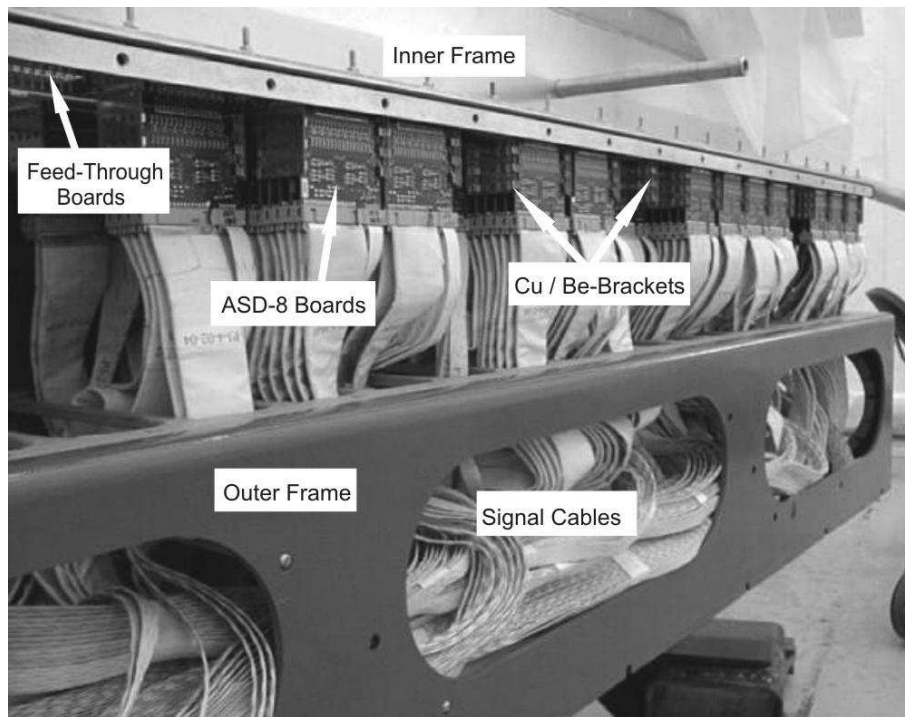


Fig. 9. Photograph of the front-end electronics on an Outer Tracker chamber: Shown is the lower part of a chamber with the ASD-8 cards plugged onto the feed-throughs at the gas box, the cables connecting the ASD-8 outputs with the TDCs and the cable frame routing the cables to the TDC crates (on the vertical frame part to the left, not visible here).

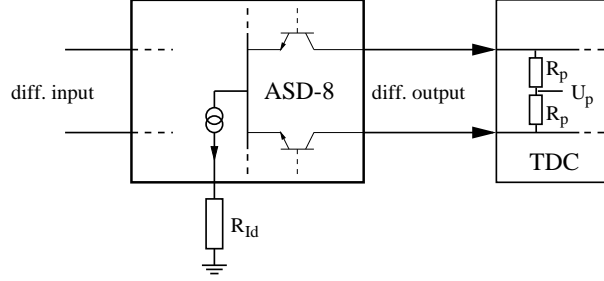


Fig. 10. Schematics of the open collector, differential output of the ASD-8; the current is adjusted by the resistor  $R_{Id}$ . The output current together with the pull-up resistors  $R_P = 62 \Omega$  and the voltage  $U_P = 1.25 \text{ V}$  determines the signal swing and the reference level of the signals.

200 or 380 mV) were used to shift the thresholds of chips or of single channels to avoid more categories or to reduce the number of rejects.

The current of the open collector, differential output of the ASD-8 is adjustable. It was chosen to yield a swing of 120 mV for the given pull-up resistors on the TDC boards (fig. 10 and Sec. 6.2). An offset of 1.25 V is added by the receivers on the TDC board. The analog outputs of the ASD-8 chips are not used.

Test pulses are capacitively coupled (1 pF) into the positive input via a 1:10 voltage divider to reduce noise pickup via the test pulse system. The pulses fire all channels on a board at the same time.

### 5.3 Low Voltage Distribution Board

The low voltage distribution board supplies 6 groups of 8 ASD-8 boards each with power, thresholds and test pulses (fig. 2). These boards are controlled by a SLIO processor (Serial Linked I/O; Philips P82C150) and are connected to the HERA-B Slow Control System via a CAN (Controller-Area-Network) bus.

On each board, two different thresholds can be set using 10 bit DACs. For each of the 6 groups one of these thresholds has to be preselected by setting a jumper. The board has an RS422 input for test pulses which can be enabled for each group separately by the CAN controller. The pulses have a length of about 30 ns; the amplitude can be adjusted by a potentiometer to a common value for each group. An internal ADC of the SLIO measures the real thresholds, supply voltages and currents using a multiplexer. The analog and digital supply voltages for each ASD-8 board are filtered by RC circuits.

## 5.4 Test and selection of ASD-8 chips and boards

### 5.4.1 Series Chip Tests and Selection

**Definition of chip quality:** HERA-B ordered a total of 90 wafers, each with about 335 chips. The yield per wafer was on average 77%. Each chip was tested according to a scheme which evaluated the general functioning, the threshold behaviour, and the noise level.

For each channel a threshold reference voltage,  $U_{ref}$ , was defined as the threshold at which a standard 4fC test pulse is recorded with 50% efficiency. The noise behaviour of a chip was characterized by the threshold  $U_{noise}$  for which the noise rate exceeded 2 kHz. The difference  $U_{ref} - U_{noise}$  is a measure for the signal-to-noise distance and thus of the quality of a channel. The parameters of the test (4fC, 2kHz) were chosen to yield a high test sensitivity in the relevant range, and to yield stable and reproducible results.

**Results of the chip test:** The chip tests revealed an appreciable range for the  $U_{ref}$  threshold (fig. 11). However, within one chip the variation of thresholds was found to be mostly much less than the  $\pm 30\%$  specified in the purchase order. The chip-to-chip variations prohibit the definition of a common threshold for the whole system keeping at the same time the overall efficiency high. On the other hand, to keep the front-end electronics simple and compact, individual threshold settings for each channel have to be avoided. As a compromise 4 categories of threshold ranges were defined:

$$U_{ref} = 850 \dots 950, 950 \dots 1050, 1050 \dots 1150, > 1150 \text{ mV}.$$

To account for the signal-to-noise variation for a given  $U_{ref}$  (fig. 11) in each of the 4 threshold categories, 3 noise categories corresponding to noise distances were defined:

$$\overline{U_{ref}} - U_{noise} = 350 \dots 450, 450 \dots 550, > 550 \text{ mV},$$

where  $\overline{U_{ref}}$  are the central values of the threshold categories ( $\overline{U_{ref}} = 900, 1000, 1100, 1200 \text{ mV}$ ). A chip was assigned to one of the 12 categories according to its minimal  $U_{ref}$  and maximal  $U_{noise}$  values. The assignment was used to mount two similar chips on a board and to combine similar boards to groups which are supplied with a common threshold.

### 5.4.2 Board Tests

The 11000 produced boards had to undergo quality tests and were then sorted according to 12 categories as was done for the single chips: 4 categories accord-

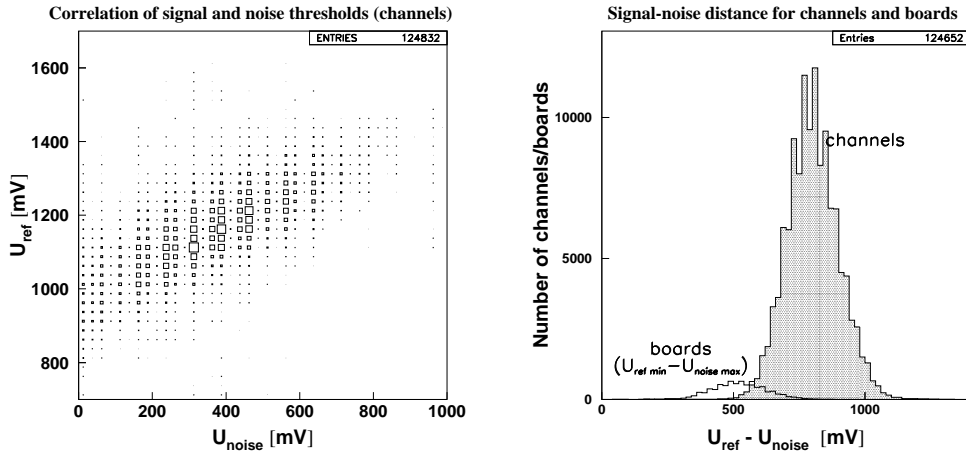


Fig. 11. Left: Threshold  $U_{ref}$  plotted against the noise threshold  $U_{noise}$  for each channel of the tested chips. Right: Distribution of the signal-noise difference  $U_{ref} - U_{noise}$  for each channel of the tested chips and for the boards where the signal-noise difference is defined by the channels with minimal  $U_{ref}$  and maximal  $U_{noise}$ .

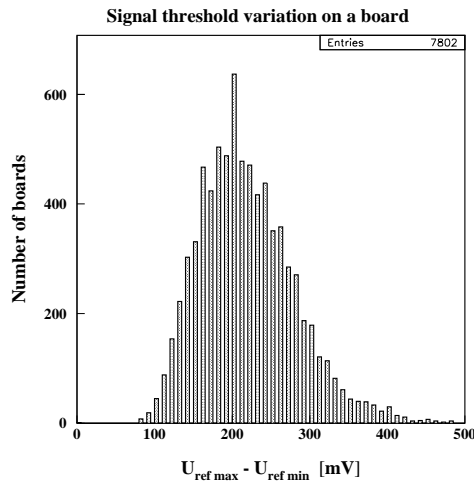


Fig. 12. Threshold uniformity on the ASD-8 boards: distribution of the difference between maximal and minimal reference threshold  $U_{ref}$  on a board ( $\sim 250$  mV/fC). Differences above 300 mV have been reduced by a diode circuit (see text).

Table 3  
 Characteristics of the TDC chip.

integration density	8 ch. on $9.4 \times 9.4 \text{ mm}^2$ die
power consumption	0.06 W / chip
operating voltage	5 V
time bin	about 0.5 ns
time resolution	about 0.2 ns

ing to the threshold reference voltage,  $U_{ref}$ , and 3 categories of signal-to-noise distance  $\overline{U_{ref}} - U_{noise}$  (see fig. 11 right). A board enters into a category according to the minimal  $U_{ref}$  and maximal  $U_{noise}$  of the channels.

Details about the distribution of the boards in different categories are given in [6]. For each board the two chips belong to the same category. The remaining variations of  $U_{ref}$  within the 16 channels can be seen in fig. 12 which shows the difference between the maximal and minimal  $U_{ref}$  on the boards. Differences larger than 300 mV have been decreased by Schottky diodes as described in section 5.2. With this procedure the threshold uniformity on the boards is about  $\pm 15\%$ . The variations between different boards are accounted for by the threshold settings on the distribution boards (section 5.3).

The board quality is mainly determined by the noise category, more than 80% are in the upper two categories with  $\overline{U_{ref}} - U_{noise} > 450 \text{ mV}$  for both chips.

## 6 The Time Measurement System

### 6.1 Introduction

The HERA-B TDC system has been developed for the readout of the Outer Tracker, the RICH, the Muon System and the High- $p_T$  Chambers. Except for the Outer Tracker the other systems use the TDC chip only as a hit register. The system is highly integrated at low power consumption and reasonable costs (Table 3).

The TDC was designed to digitize the time in 0.5 ns bins with an 8 bit output. After digitization the data of each channel is stored in a 128 cells deep digital pipeline which is read out by a digital signal processor (SHARC processor ADSP-21060 from Analog Devices). With the integrated channel buffering the requirement of a dead-time free readout after the First Level Trigger decision is fulfilled.

### 8 channel TDC / 64 channel HIT chip

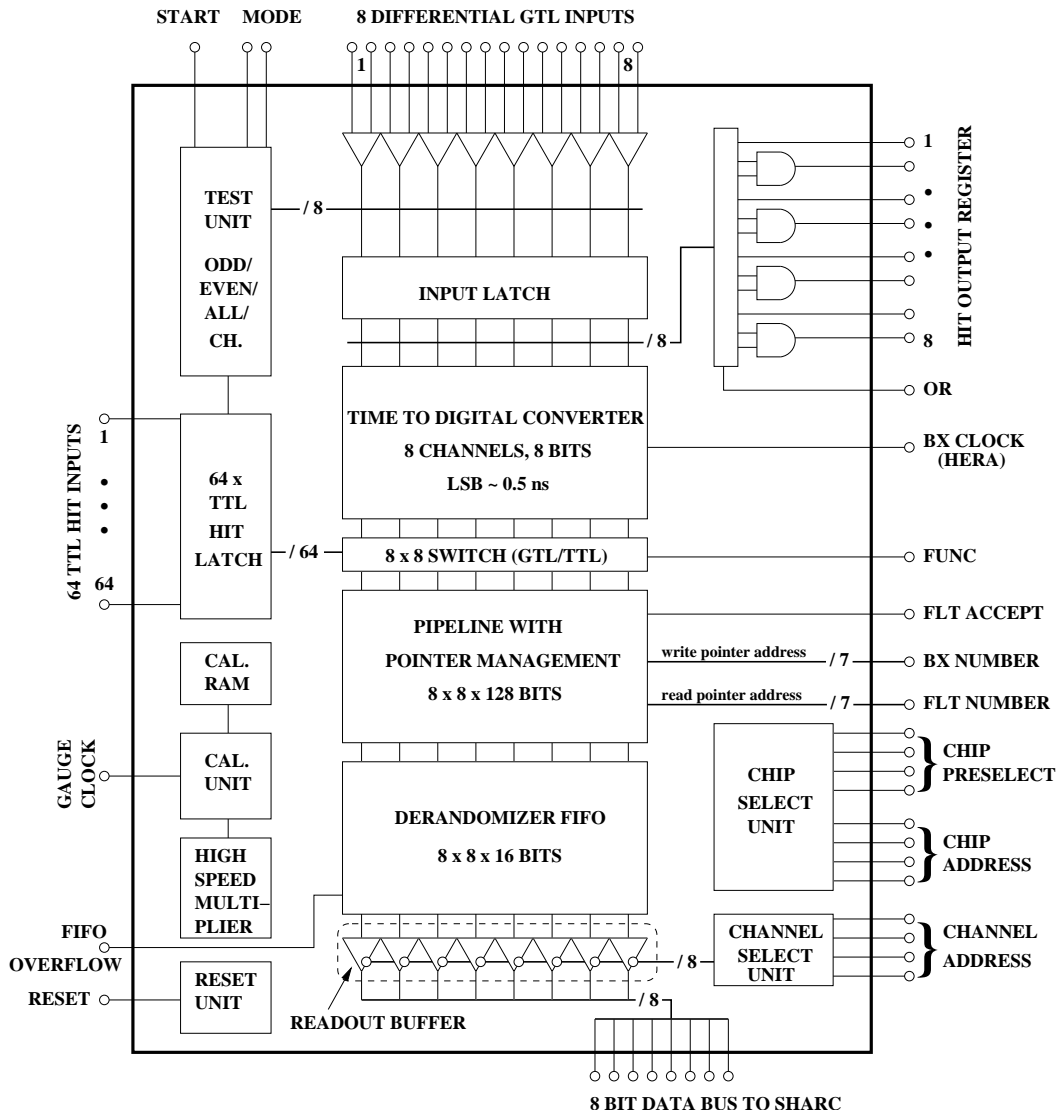


Fig. 13. Block diagram of the TDC chip.

The chips are mounted on boards with 16 chips each, corresponding to 128 TDC channels per board. The crates housing the TDC boards are mounted on the cable frame of the detector superlayers, except for the magnet chambers for which the TDC crates are placed outside the magnet. The maximal cable length between the ASD-8 boards and the TDC crates is 5 to 10 m, depending on the superlayer.

## 6.2 *The TDC Chip*

### 6.2.1 *Overview of the Layout*

Figure 13 shows the structure of the TDC chip which was designed by the company MSC<sup>8</sup> and produced by the company NEC (Japan). The chip was developed as an ASIC (Application Specific Integrated Circuit) in 0.8  $\mu\text{m}$  CMOS technology using VLSI (Very Large Scale Integration) design techniques (process provider: NEC). The  $9.4 \times 9.4 \text{ mm}^2$  die is housed in a 160 pin-package. The TDC chip includes the following features:

- 8 differential inputs for the ASD-8 outputs,
- 8 hit output registers (with optional OR for neighbouring channels) for the First Level Trigger,
- 8 x 8 bit time-to-digital converter,
- calibration unit (with high speed multiplier),
- buffer memory pipeline,
- derandomizer FIFO memory,
- readout buffer with addressing unit,
- chip and channel select units,
- test device for all input signals,
- hit input register for 64 channels.

### 6.2.2 *Input Circuit*

The differential input signals from the ASD-8 chips are received by a GTL-I/O-Interface (GTL = Gunning Transceiver Logic). The GTL standard, characterized as a low-level, high-speed, noise-immune digital logic, requires the differential swing to be  $\geq 50 \text{ mV}$ , in the Outer Tracker system it was set to 120 mV. The levels are defined by the circuit on the TDC board as shown in fig. 10. All other input/output signal levels of the chip are TTL compatible to simplify interfacing.

After passing the GTL-I/O-Interface the drift chamber signals are latched

---

<sup>8</sup> MSC, Industriestr. 16, D-76297 Stutensee, Germany

with the BX clock. Thus the hit information is available in the hit output register in the next BX clock cycle and can be used by the First Level Trigger. If required, the hit information of two neighbouring channels can be merged by an OR-function.

### 6.2.3 TDC Circuit and Internal Calibration

The heart of the TDC chip is an 8 bit TDC circuit which converts time differences into digitized values using a delay line chain made of logic gates. The method<sup>9</sup> [7] is fully digital with the major advantage that no conversion time is required and the measurements can be made nearly without deadtime (section 6.4). The time measurement bin of the circuit follows from the basic gate delay and was measured to be about 0.48 ns, very close to the targeted 0.5 ns.

Each chip has nine channels, eight for time measurements and one for calibration (not shown in fig. 13). At the startup of the system (after a Reset) all nine channels are calibrated assuming a linear relation between the measured time interval and the TDC output (see section 6.4). For each channel, slope and offset of a straight line are determined by measuring time intervals of 100 ns and 200 ns, both derived from a 10 MHz gauge clock, with a 10 bit resolution. The straight line parameters include a mapping of a 100 ns interval onto the 256 output counts of the TDC. The two parameters for each channel are written into the memory of the calibration unit.

To compensate temperature and voltage variations the chip features a self-calibration procedure. During data taking, every 0.8 seconds the slope parameter of the calibration channel is re-measured in the same way as for the initial calibration and a correction factor is calculated which is also written into the memory of the calibration unit. The time for the other 8 channels on the chip is multiplied by this factor. The mapping of the 100 ns interval onto 8 bits including the multiplication by the correction factor is done during the transfer from the pipeline to the derandomizer by the High Speed Multiplier unit.

The time is measured in common stop mode. The pulse from the GTL input or the test device yields the START while the STOP is derived from the external HERA BX clock which is synchronized with the bunch crossing signal (BX). Because of the mapping of 100 ns onto the 8 bits (256 counts) the least significant bit (LSB) of the time measurement (1 TDC count) corresponds to 0.39 ns in HERA-B. Note that the bins for the time measurement remain fixed at about 0.48 ns which determines the time resolution (section 6.4).

---

<sup>9</sup> German patent nr. 41 11 350



#### 6.2.4 *Buffer Circuits*

The pipeline of each channel is a ring-buffer memory with 8 bits per cell and a depth of 128 events. The pipeline depth corresponds to a time interval of about 12  $\mu$ s available for the First Level Trigger decision. Writing and reading the data is controlled by two different pointers using the BX number as address. On an Accept signal from the First Level Trigger (FLT Accept) the Fast Control System (FCS) generates the read pointer (FLT Number) and pushes the event data to the derandomizer FIFO. The design mean trigger rate is 50 kHz although the TDC system is capable to run at more than 100 kHz. The derandomizer FIFO with a depth of 16 events serves for each TDC channel as buffer memory for peak rates. The events in the FIFO are read out into the Second Level Buffer (system of SHARC processors).

The readout is organized by the Chip Select Unit which addresses the TDC chip and the Channel Select Unit which addresses the buffer of each channel. If the readout cannot follow the trigger rate the FIFO is filled up and the next event could be lost. In this case a FIFO Overflow bit is set which is used in HERA-B to stop the data acquisition until the buffer is available again.

#### 6.2.5 *Control and Test Functions*

The chip can be tested using an internal pattern generator which is controlled by a 3 bit input for setting the test functions. Two bits control the mode (all, even, odd channels on) and one bit starts the measurement of a preselected time interval provided by the FCS system. In this way the proper functioning of the chip can be tested.

Instead of the use as 8 channel TDC, the chip can also be used as a hit register with 64 channels. The hit register mode is set by a function bit (FUNC) which enables the 64 hit inputs and switches off the TDC circuits. The hit inputs are grouped by 8, so that the same data format (8 times 8 bits) can be used. The buffer management is the same as for the TDC application.

### 6.3 *The TDC board*

The TDC board (fig. 14), built in 9U VME format, comprises 16 TDC chips together with a DAQ interface (SHARC Link). Except for the GTL inputs the signals on the board are TTL levels. On the boards to be used as a hit register, an auxiliary chip converts the differential amplifier outputs into single ended lines ('64 TTL HIT INPUTS' in fig. 13). All channels can be initialized in parallel by a general Reset.

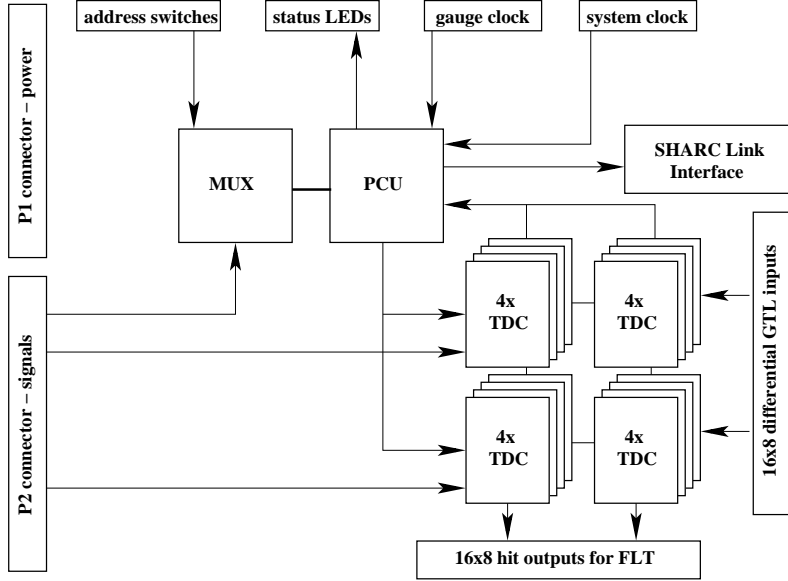


Fig. 14. Schematics of the TDC board structure for time measurement.

The main components on the TDC board are:

- 16 TDC chips,
- SHARC Link interface,
- system clock + gauge clock (reference clock for calibration),
- Protocol Control Unit (PCU) + multiplexer (MUX),
- address switches (board and chip addresses).

The high-speed SHARC Link interface on the board (mainly fast drivers and transfer logic) transfers the data for all channels from the FIFO on the TDC chip via its point-to-point connection to a host system which, in HERA-B, is a SHARC processor. The 6-bit link port used for the transfer has four data lines, a clock line and an acknowledge line. The link ports send data packed into 48 bit words in direct communication with the SHARC memory. A fixed clock/acknowledge handshake has been designed to control transfers (only transmit cycles) to a SHARC-compatible receiver.

The Protocol Control Unit (PCU), which is a programmable logical device (Lattice Semiconductors ispLSI 1048E), was employed to address all TDC channels sequentially by using the Chip and Channel Select and perform a packet-oriented protocol transmission consisting of 144 bytes. This Event Format Block Protocol is organized in three major sections: the header field, the data field and the trailer field (for details see [8]).

The system clock determines the execution and transmission rates. The TDC board can utilize clock rates from 10 MHz to 30 MHz. Thus the maximal transfer rate to the SHARC board is 15 MByte/s (4 bit data line at 30 MHz). In the Outer Tracker system a 27 MHz clock is used. A small clock circuitry

Table 4

Environmental and electrical specifications of the TDC board.

Operation temperature range	0 to 55 °C	
Operation humidity range	0 to 90 %	
Height	366.8 mm	(9 VME HU)
Depth	220.0 mm	
Width	1.9 mm	
Weight	736 g	
<b>Voltage</b>	<b>Regulation</b>	<b>Max. Current</b>
+5 V (digital)	±5%	3.02 A
+5 V TDC	±5%	1.18 A

generates a gauge clock rate of 10 MHz to be used for the TDC online calibration.

The status of the TDC board is displayed by four LEDs indicating a System Reset, a possible overflow situation, a Trigger Accept and a fault condition. The overflow signal is a logical OR signal of all TDC overflow flags.

To limit noise on the ground plane the TDC board provides three separate, independently grounded power systems: for the digital control, for the TDC chips and for the FCS signals and the SHARC outputs. The user can select the optimal power scheme by bridges connecting planes at several locations on board. For the HERA-B application one common power supply turned out to be sufficient. The major environmental and electrical specifications of the board are summarized in Table 4.

#### 6.4 Calibration and Performance of the TDC system

The TDC system was designed to have a time measurement binning of about 0.5 ns with a differential non-linearity of less than 3%. Due to tolerances in the production process the actual value can differ from the design value. The time bin size was measured for an engineering sample of 20 TDC chips with a chip tester HP 82000 yielding  $(0.48 \pm 0.05)$  ns at the working temperature of 35 °C with a temperature dependence of  $(0.0015 \pm 0.0007)$  ns/K. The quoted errors include the uncertainty of the measurement device and the dispersion of the sample. For all delivered charges of chips random test samples have verified that these values remained stable. Because of the mapping of the required maximal time interval onto 8 bits by the calibration procedure described in section 6.2, the actual size of the time measurement bin is uncritical. It has

only to be assured that the maximal time interval to be measured can be covered with 8 bits (i. e. the time corresponding to the LSB of the TDC output cannot be larger than time measurement bin).

All TDC boards were tested for linearity, dead time and time resolution. A dead time was measured to arise between sequential BX clock cycles with typical values between 3 ns and 5 ns. This decreases only slightly the maximally measurable time interval.

The linearity of the time measurement was verified for the whole time range of 100 ns. A straight line fitted to the measured TDC values over a range of 100 ns yields a slope of  $(2.560 \pm 0.002)$  counts/ns reflecting the mapping of the time range onto 256 bins. The error is determined from fitting time measurements of a single channel.

The resolution for a single TDC channel was measured to be 0.14 ns (1 standard deviation), in agreement with the statistically expected value for a time measurement in steps of 0.48 ns. The corresponding uncertainty of the hit position of  $11 \mu\text{m}$  contributes negligibly to the position resolution of the detector. The long-term stability of the resolution is assured by the periodic calibration every 0.8 s. Variations on a shorter time scale could be caused by ripples from the TDC power supplies. The measured resolution confirms that the chosen power supplies are appropriate.

More details on the calibration of the TDC channels and the performance of the TDC system can be found in [8].

## 7 Electronics Installation and Commissioning

### 7.1 Installation and System Integration

The ASD-8 boards of the different categories were installed such that for the innermost detector regions with the highest occupancies amplifiers with a large signal-noise difference ( $> 550 \text{ mV}$ ) were chosen. The outer detector parts, contributing less to the acceptance, were equipped with boards with a small signal-noise difference. The CAN bus controlled distribution boards allow to set individual thresholds for groups of 8 ASD-8 boards (see section 5.3).

The grounding and shielding scheme of the front-end electronics has been implemented as described in section 3.3. After the initial installation some rework had to be done to improve the system stability. For example, bad

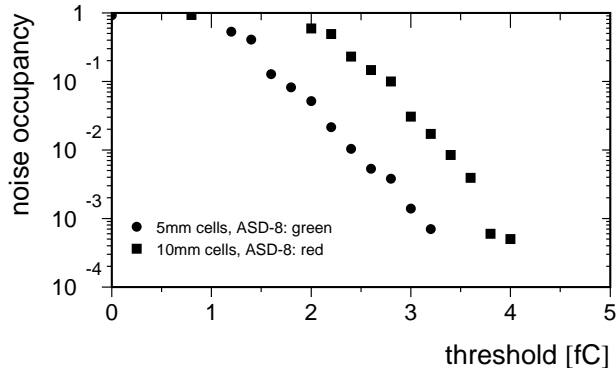


Fig. 15. Noise occupancies for two different sectors of a superlayer after installation in HERA-B: The 5 mm cells are equipped with ASD-8 boards from the best noise category, labelled as “green” (circles), while the 10 mm cells are connected to boards of the worst noise category, labelled as “red” (boxes).

ground connections between either amplifier and gas box or amplifier and cable shielding led to oscillations of the amplifiers with their characteristic frequencies of 40 to 80 MHz.

Another problem was a high noise level generated by the signal connections between the TDC boards and the trigger link boards which prepare the tracker hits for the First Level Trigger. This forced an increase of the thresholds for the superlayers providing the trigger input. To overcome this problem, high frequency filters were added and the current transfer over these lines was reduced by removing the line driver chips from the affected TDC boards. In this way the thresholds could be set to similar values as in the other superlayers.

## 7.2 Commissioning and Performance

The described front-end electronics has been used in HERA-B since 1997, the beginning of prototype tests, and since January 2000 all tracker channels were fully equipped. They were running until the end of data taking of the HERA-B experiment in 2003 with a very low failure rate, with the exception of intermediate problems with the HV boards as described below. For example, only about 0.1% of the TDC boards and even less of the ASD-8 boards had to be replaced.

The noise occupancies (probability to find a noise hit in the readout time window) for two sectors of a superlayer after installation in HERA-B are shown in fig. 15. The plot shows a sector with 5 mm cells equipped with ASD-8 boards with low noise thresholds and a sector with 10 mm cells and ASD-8 boards from the worst noise class. For the best ASD-8 boards the threshold can be set as low as 2 fC, while for the worst category the threshold has to be increased

to about 3 fC to achieve a similar noise occupancy around 1 %.

In the beginning of 2000 the HERA-B detector was completed and took first data from April to August. Unfortunately the expected performance of the Outer Tracker system could not be reached during this run. The most severe problem was a continuous loss of channels due to high voltage breakdowns until finally 15% of the channels were lost.

During the shutdown of HERA from autumn 2000 to summer 2001 major repair and improvement work on the Outer Tracker had solved all remaining problems. In particular, most of the high voltage breakdowns could be identified to be due to two specific capacitors on the HV board. These two were soldered with a different technique than the rest, since they were placed on the opposite side of the HV boards (section 4.1). While 15 capacitors were glued prior to the soldering process, the remaining two were positioned directly on the board and soldered. It seems that the remaining soldering paste under these two capacitors increased the probability of high voltage breakdowns across them. About 12000 of these capacitors had to be replaced. This required access to every module and hence a complete disassembly of the detector which was quite manpower and time consuming.

After these repairs the Outer Tracker reached its final status. In the data taking period 2002/2003 the detector was operated without any specific problems. The design goals of the readout electronics have been mostly reached. A slight deterioration of performance was introduced by the necessity to raise the thresholds in some parts of the detector as explained above. This deficit is mainly caused by the relatively large channel-to-channel variations of the ASD-8 sensitivity and noise performance and could probably have been overcome by applying individual thresholds for each channel. In retrospective, the drawbacks of the grouping of thresholds seem to preponderate the advantages of simplicity.

It was demonstrated that the electronics can handle high rates, up to the design value of 40 MHz interaction rate with an occupancy in the hottest channels of more than 20%. However, finally the experiment was mostly run at rates not exceeding 5 MHz.

The analysis of the 2002/2003 data yielded an overall good performance of the Outer Tracker, with a high tracking efficiency of 96% and a track hit resolution of 370  $\mu\text{m}$  for tracks above 5 GeV. The resolution is much worse than the design value. This is partly due to the not optimal threshold settings, as described above, but also to deficiencies in the calibration and alignment procedures. Details of the Outer Tracker performance are described in a separate paper [9].

## 8 Summary

In this paper we have described the front-end readout system for the 112674 drift chamber channels of the HERA-B Outer Tracker detector. The basic components are the amplifier-shaper-discriminator chip ASD-8 and a customized TDC chip which provide the required high integration density, low noise, high sensitivity, rate tolerance, and low per-channel cost.

The high sensitivity of the ASD-8 amplifiers together with a large chip-to-chip variation of the thresholds was a major challenge for the implementation of the amplifiers. Grouping the chips according to threshold and noise categories an economic system of threshold setting was developed leading to an acceptable noise performance for the whole system. An improvement is still possible by an individual adjustment of the thresholds for each channel.

The TDC system is based on an ASIC which digitizes times in bins of about 0.5 ns within a full scale of 256 bins. The time measurement is very stable due to an internal automatic calibration procedure. In HERA-B the drift times are measured within every bunch crossing period of 96 ns with respect to the external HERA clock. An integrated pipeline stores data for 128 events satisfying the requirement for a dead-time free trigger and data acquisition system at the design trigger rate.

The prototype tests and the analysis of data taken with the full detector show that the front-end electronics of the Outer Tracker fulfills the requirements posed on the detector for running in a high rate environment.

## Acknowledgements

We thank our colleagues of the HERA-B Collaboration who made in a common effort the running of the detector possible. The HERA-B experiment would not have been possible without the enormous effort and commitment of our technical and administrative staff. It is a pleasure to thank all of them.

We are grateful to Mitchell Newcomer for discussions and many technical advices and to Karl-Tasso Knöpfle for carefully reading the manuscript and for useful comments.

We express our gratitude to the DESY laboratory for the strong support in setting up and running the HERA-B experiment. We are also indebted to the DESY accelerator group for the continuous efforts to provide good beam conditions.

## References

- [1] E. Hartouni et al., HERA-B Design Report, DESY-PRC 95/01 (1995).
- [2] F.M. Newcomer et al., IEEE Trans. Nucl. Sci. NS-40 (1993) 630; H.H. Williams et al., Nucl. Instr. and Meth. A360 (1995) 146.
- [3] H. Albrecht et al. (HERA-B Outer Tracker Group), ‘The Outer Tracker Detector of the HERA-B Experiment, Part I: Detector’, to be published in Nucl. Instr. and Meth. A.
- [4] M. Dam et al., Nucl. Instr. and Meth. A525 (2004) 566.
- [5] <http://www-hera-b.desy.de/subgroup/detector/tracker/outer/electronics/docu.html>
- [6] K. Berkhan et al., ‘Large System Experience with the ASD-8 Chips in the HERA-B Experiment’, Proceedings of the 5th Workshop on Electronics for LHC (Snowmass, Colorado, USA 20 - 24 September 1999), CERN 99-09, CERN/LHCC/99-33, p. 564.
- [7] R. Geiges and K. Merle, ‘A High Resolution TDC Subsystem’, IEEE Trans. Nucl. Sci. Vol. 41-1 (1994) 232.
- [8] R. Zimmermann, ‘Zeitmesselektronik für den HERA-B Detektor’ (in German), Doctoral thesis, Universität Rostock (1999), unpublished, [http://www-hera-b.desy.de/general/thesis/diss/diss\\_raoul\\_zimmermann.ps.gz](http://www-hera-b.desy.de/general/thesis/diss/diss_raoul_zimmermann.ps.gz).
- [9] H. Albrecht et al. (HERA-B Outer Tracker Group), ‘The Outer Tracker Detector of the HERA-B Experiment, Part III: Performance’, to be published in Nucl. Instr. and Meth. A.